

Supporting Information

Geminal-Cu Catalysts Drive Efficient C-C Coupling to Boost Ethylene Production via Electrochemical CO₂ Reduction

Hisham G. El-Aqapa, Ghada E. Khedr, Ibrahim M. Badawy[†], Ahmed M. Agour[†], Abdelrahman M Abdelmohsen, and Nageh K. Allam*

Energy Materials Laboratory (EML), Physics Department, School of Sciences and Engineering,
The American University in Cairo, New Cairo 11835, Egypt.

* Corresponding Author's email: nageh.allam@aucegypt.edu

[†] Equal Contribution

Experimental section

Materials preparation

Synthesis of exfoliated PCN. Bulk PCN was synthesized by heating urea in a crucible at 550 °C, with a heating rate of 2 °C.min⁻¹, for a duration of 3h under static air conditions. Exfoliated PCN was obtained through thermal exfoliation at 500 °C, with a heating rate of 5 °C.min⁻¹, for a period of 5 hours under static air. The exfoliation process was repeated multiple times until efficient exfoliation of PCN was achieved.

Synthesis of Cu_g-PCN catalyst. Cu_g-PCN was synthesized using an ion exchange method, following the previously reported procedure. Initially, exfoliated PCN and a CuCl₂ precursor were dispersed in a formamide solvent and subjected to sonication for 30 min. Subsequently, the mixture was vigorously stirred in an oil bath at 120 °C for a duration of 12h. The resulting mixture was then subjected to centrifugation, followed by multiple washes with ethanol and drying at 80 °C for 6h. Finally, the obtained powder was heated at a ramping rate of 2°C.min⁻¹ under a N₂ atmosphere at 500 °C for 5h.

Synthesis of Cu_i-PCN catalyst. Cu_i-PCN was synthesized using a stepwise ligand removal approach¹. First, CuCl₂ and exfoliated PCN were mixed together in a (20 ml) ethanol solution and sonicated for 10 min. The mixture was dried in an oven at 50 °C and subsequently heated to 450 °C in a nitrogen atmosphere, with a heating rate of 5 (°C.min⁻¹). This heating process lasted for 5h. Afterwards, the powder was carefully washed using a mixture of water and ethanol, and then dried again in an oven at 80 °C. Ultimately, the powders were heated to 550 °C at a rate of 2 (°C.min⁻¹) and kept under a flow of nitrogen for 5 h to ensure their protection.

Material characterization

Powder XRD analysis was implemented via a D8 Discover (Bruker). The morphology of the samples was investigated by scanning electron microscope (SEM, Model JSM-760F). TEM imaging and selected area electron diffraction (SAED) studies were carried out using Talos-F200i TEM. The elemental composition of the surface and the valence states of the samples were analyzed through X-ray photoelectron spectroscopy (XPS) with Al K α radiation. Inductively Coupled Plasma - Mass Spectrometry was carried out to quantify the metal loading wt% using (ICP-MS) NexION 1000 ICP-MS.

Electrochemical measurements and setup

The electrochemical measurements for CO₂ reduction were conducted using an H-cell design inspired by Dr. Kuhl's. The H-cell comprises two acrylic plates, each with a working area of 8x8mm for placing the anode and cathode materials. A Nafion 117 membrane is placed between the two plates, and a reference electrode is inserted through a hole in the cathode compartment. CO₂ gas with a purity of 99.999% is introduced into the H-cell from the bottom at a controlled flow rate of 50 standard cubic centimeters per minute (scm) using a mass flow controller (MFC). The product gas is directed towards the inlet valve of gas chromatography (GC), where it is

analyzed at set intervals of 13 minutes, 32 minutes, and 55 minutes with a total runtime of 60 minutes for each run. A Biologic SP300 type potentiostat/galvanostat was used for all electrochemical experiments with a 3-electrode set-up in the acrylic cell. The three-electrode system involved a counter electrode of Ru/C ink deposited on Ni foam, and Ag/AgCl (KCl sat.) as a reference electrode. The cathode (the catalyst ink deposited onto 1x1cm graphite sheet), reference electrode (Ag/AgCl saturated with KCl), and anode (Ru/C ink deposited on Ni foam) were employed, while 0.1 M KHCO₃ and 0.1 M KOH electrolytes were used for the cathode and the anode compartments, respectively. through the electrochemical cell. The applied potentials were adjusted with post-measurement iR drop correction, considering an average uncompensated resistance (R_u) of 86 Ω , determined through electrochemical impedance spectroscopy at 100 kHz. The gas products generated during the electrolysis were analyzed using an online gas chromatography (SRI 8610C Multi-gas #5, 6' Haysep D and 6' Molecular Sieve 5A) equipped with thermal conductivity and flame ionization detectors. All current densities were normalized to the geometric area of the working electrode (1 cm²).

Cyanide adsorption and *in situ* quantification of active sites

Caution: *It is of utmost importance to exercise caution and follow strict safety protocols when conducting experiments involving cyanide or similar substances. We strongly recommend that all cyanide-related experiments be performed within a fume hood or in a well-isolated environment such as a glovebox. Additionally, researchers must wear HCN detectors throughout the experiments to prevent any inhalation of hydrogen cyanide (HCN) gas. It is strictly prohibited to directly add KCN powder to an acid solution. These guidelines provide comprehensive instructions and precautions to ensure the safety of researchers and minimize potential risks.*

Cyanide adsorption was performed using a two-compartment electrochemical H-type cell. The cell was equipped with a Nafion 117 membrane, which effectively separated the working electrode from the counter and reference electrodes. For the working and counter electrodes, graphite rods were utilized, while an Hg/HgSO₄ electrode served as the reference electrode. The

aqueous cyanide solution was prepared by dissolving KCN ($\geq 96\%$ purity, Sigma-Aldrich) in deaerated ultrapure water. To prevent any unwanted dissolution of oxygen in the electrolyte and subsequent competitive adsorption of oxygen on the samples, the cyanide poisoning experiments were conducted within an argon-filled chamber. Initially, the catalyst powder (30 mg) was dispersed in the electrolyte and mechanically stirred using a magnetic bar at a rotation speed of approximately 300 rpm to prevent sedimentation. Prior to analysis, any dissolved oxygen in the electrolyte was removed by purging with argon for 30 minutes at the open-circuit potential (OCP). After 10 minutes of stabilization at a specific potential (typically $-0.6 V_{\text{HgSO}_4}$ to prevent Cu^+ oxidation), an aqueous cyanide solution (8 mM) was injected into both compartments, and the initial concentration of CN^- ions was adjusted to 200 μM . Catalyst poisoning was then carried out for 15 minutes at the same potential used during the stabilization step. The compartment was fully closed without any gas purging to prevent the loss of cyanide via degasification of $\text{HCN}(\text{aq})$. The change in CN^- ion concentration was measured in the filtered electrolyte after dilution with deionized water (electrolyte-to-water volume ratio of 1:19). Cyanide concentration in the electrolyte was measured using the indophenol blue method. The diluted electrolyte (2 mL) was combined with 2 mL of a 1 M NaOH solution containing salicylic acid (5 wt%) and sodium citrate (5 wt%). Subsequently, 1 mL of 0.05 M NaClO and 0.2 mL of sodium nitroprusside ($\text{C}_5\text{FeN}_6\text{Na}_2\text{O}$ (1 wt%)) were added. The absorbance at a wavelength of 655 nm was measured to calculate the concentration of indophenol blue. To establish a calibration curve correlating concentration with absorbance, various amounts of a standard KCN solution were employed. The oxygen reduction reaction (ORR) activity of the poisoned catalyst was then measured to determine the difference in current density (j) values between the pristine and poisoned catalysts, denoted as Δj .

Computational methods

Quantum-chemical studies were conducted using Kohn–Sham DFT within the framework of periodic DFT methodology. This approach offers extensive data for analyzing geometric structures, and catalytic mechanisms. Periodic DFT calculations were conducted using the Vienna Ab initio Simulation Package (VASP). First-principles calculations utilizing spin-polarized Kohn–Sham formalism were conducted for structure optimizations and reaction mechanisms. The calculations employed the generalized gradient approximation from the Perdew–Burke–Ernzerhof exchange-correlation functional, the projector-augmented wave method, and a plane-wave basis set with a cutoff energy of 500 eV. A convergence criterion was established at 0.01 eV Å⁻¹. A vacuum layer of 17 Å was incorporated in the z direction to prevent artificial interactions between adjacent images. All calculations utilized a 4 × 4 × 1 k-point sampling method. A 2 × 2 supercell of the PCN structure was utilized to model the geminal and isolated copper. The adsorption energy is expressed as

$$E_{ads} = E_{adsorbed} - E_{aseparated}$$

indicating that stronger adsorption corresponds to a more negative adsorption energy.

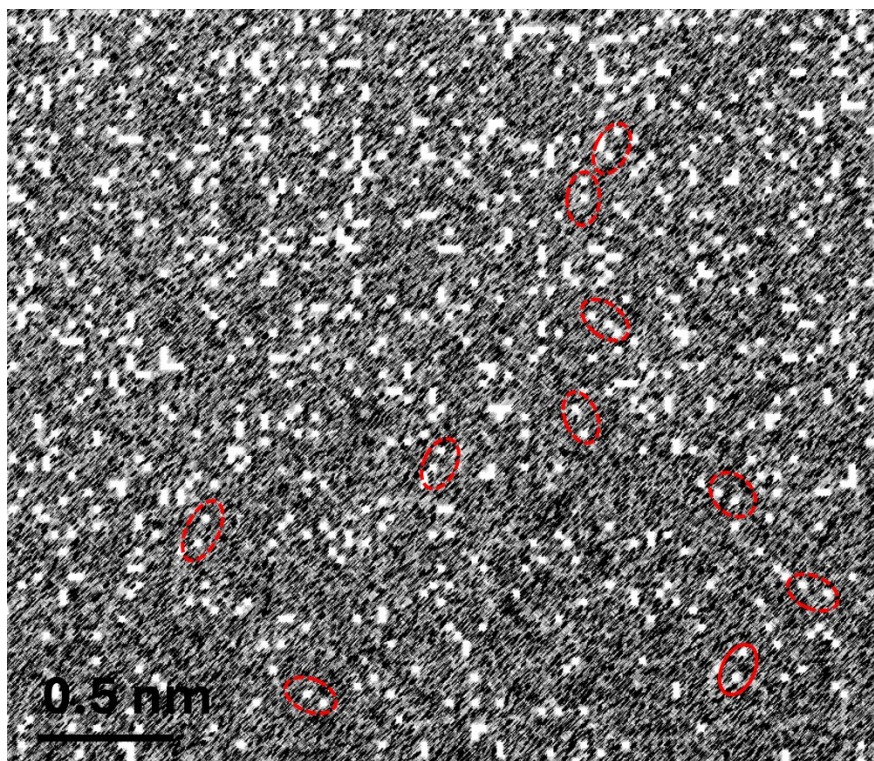


Figure S1. HAADF-STEM image of Cu_g-PCN.

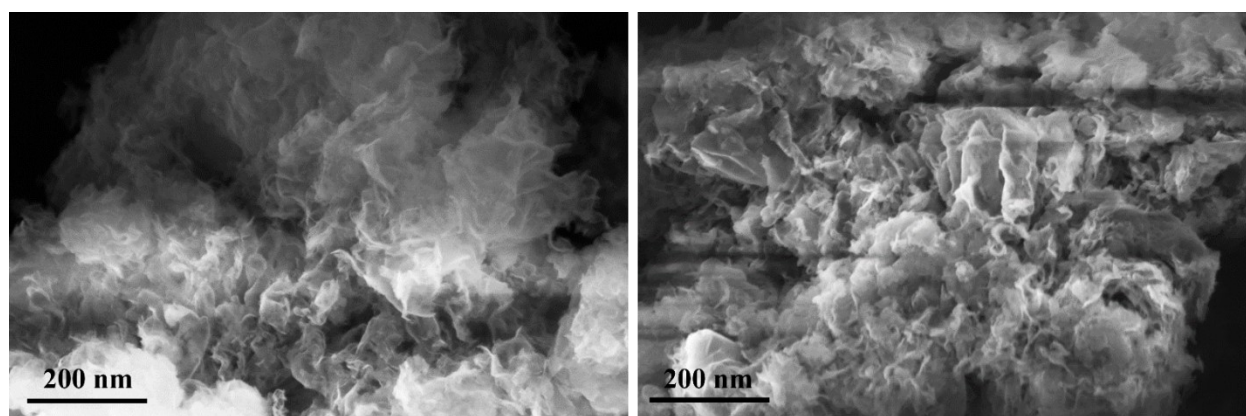


Figure S2. SEM of Cu_g-PCN.

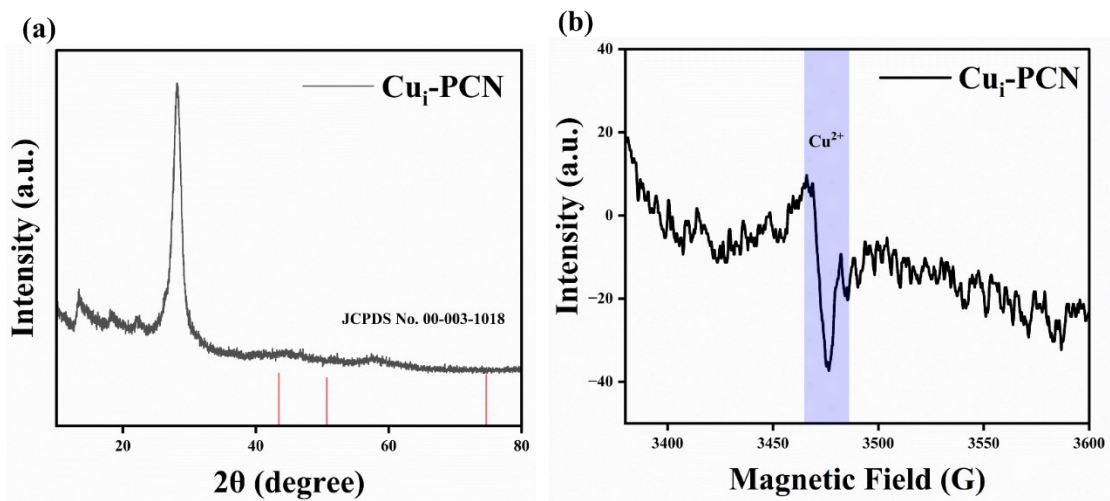


Figure S3. (a) XRD of Cu_i-PCN (b) EPR spectrum of Cu_i-PCN.

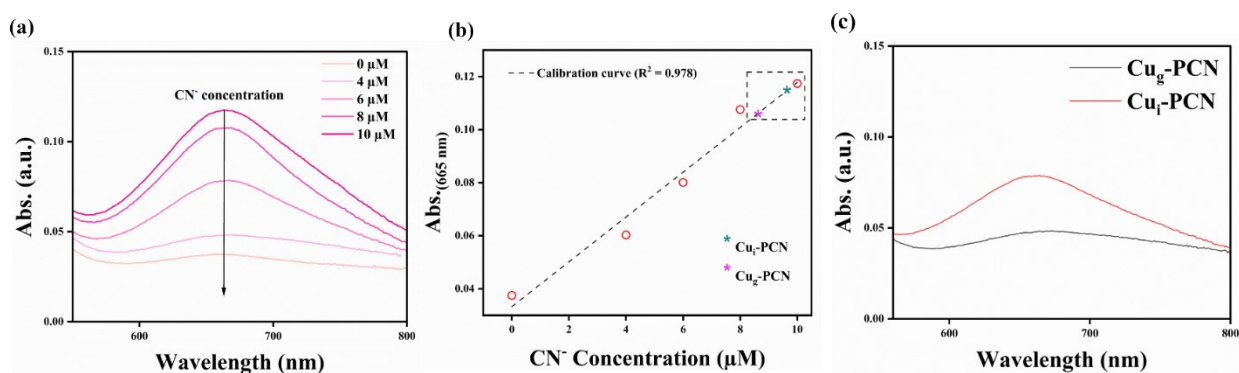


Figure S4. (a) UV-VIS spectrum of different diluted concentrations of CN⁻ (0-10 μM) (b) Calibration curve for quantification of the amount of adsorbed CN⁻ on the metal sites. (c) UV-vis spectrum of DI water used for rinsing the catalysts after the cyanide adsorption experiment.

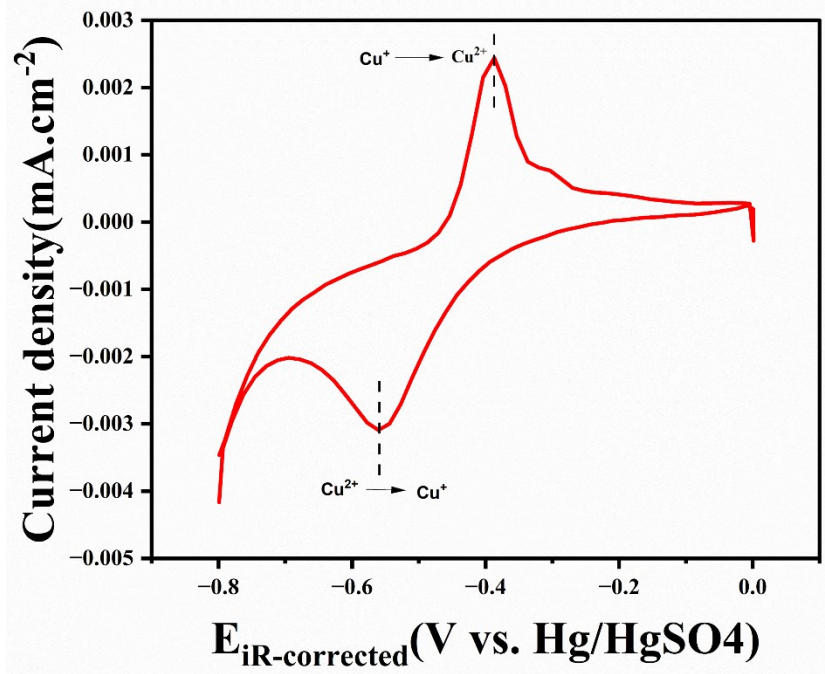


Figure S5. (a) Cyclic voltammogram of $\text{Cu}_g\text{-PCN}$ in 0.1 M HClO_4 .

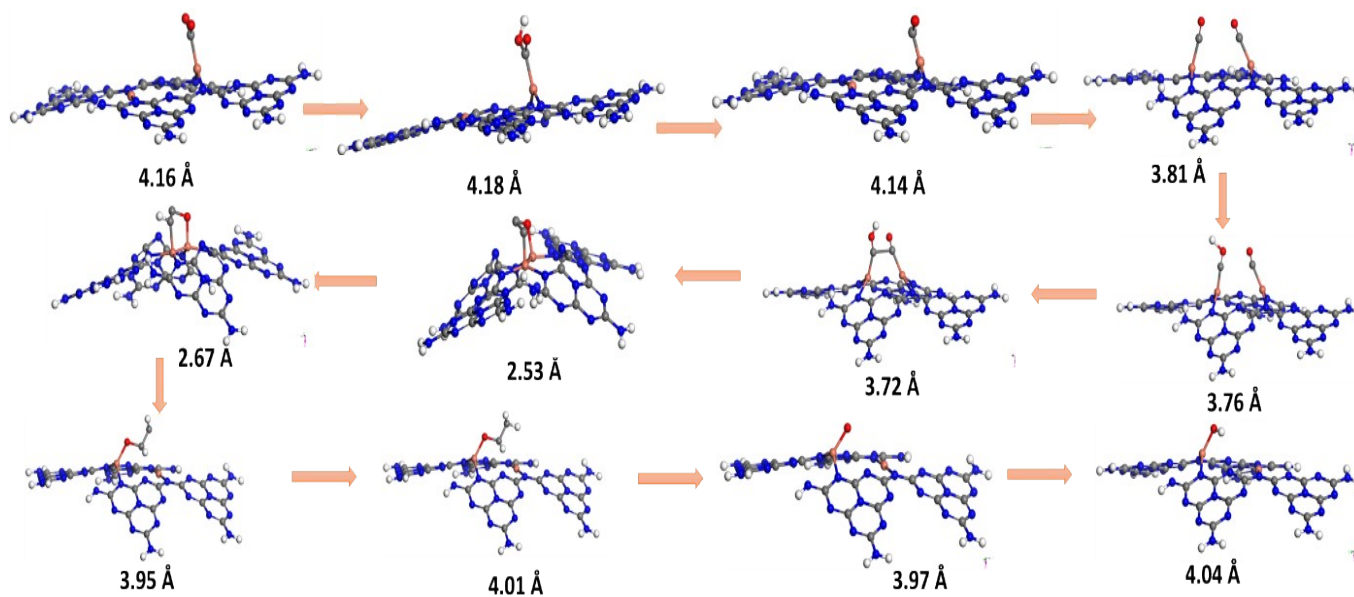


Figure S6. The reaction mechanism of CO_2RR on geminal Cu atoms, including the dynamic Cu–Cu distance for each intermediate.

Table S1. Faradaic efficiency of the different products for Cu_g-PCN and Cu_i-PCN catalysts.

Potential (V vs. RHE)	FE(%) C ₂ H ₄	FE(%) CO	FE(%) CH ₄
Cu_g-PCN			
-0.8	4.1365	1.1736	0.3648
-0.9	8.1367	3.33615	0.41324
-1	11.13745	4.21435	0.42652
-1.1	20.2253	3.35614	0.51349
-1.2	17.1567	3.1249	0.35468
Cu_i-PCN			
-0.8	2.3564	1.7604	0
-0.9	4.2153	4.00338	0
-1	5.2471	8.864395	0.1579
-1.1	9.3641	5.891754	0.13241
-1.2	7.5354	4.3214	0.03472

Table S2. Comparison of SACs in the literature and their performance towards ethylene production.

Catalyst	Electrolyte	Cell type	Applied potential	Faradic efficiency of C ₂ H ₄	Partial current density for C ₂ H ₄	Ref
BNC-Cu	0.5M KHCO ₃	Semi-flow cell	-1.59 vs RHE	6.11%	33.61 mA/cm ²	2
Cu-C-N-900	0.1 KHCO ₃	H-cell	-1.6 vs RHE	10.5%	3.63 mA/cm ²	3
CuCo 1%	1M KHCO ₃	Flow cell	-1.1 vs RHE	14.1%	≈200 mA/cm ²	4
PA-CuDBC-1	0.5 KHCO ₃	H-cell	-1.1 vs RHE	7.1%	2.6 mA/cm ²	5
Cu-PHI	1M KOH	Flow cell	-0.84 vs RHE	10 %	50 mA/cm ²	6
Cu SA/R-GDY	1M KOH	Flow cell	-1.2 vs RHE	≈ 5 %	12 mA/cm ²	7
Cu _g -PCN	0.1M KHCO ₃	H-cell	-1.1 vs RHE	20.1%	1.5 mA/cm ²	This work

References

1. X. Hai, S. Xi, S. Mitchell, K. Harrath, H. Xu, D. F. Akl, D. Kong, J. Li, Z. Li, T. Sun, H. Yang, Y. Cui, C. Su, X. Zhao, J. Li, and J. Pérez-Ramírez, *Nat. Nanotechnol.*, 2022, 17, 174–181.
2. Dai, Y. *et al.* Manipulating local coordination of copper single atom catalyst enables efficient CO₂-to-CH₄ conversion. *Nat. Commun.* **14**, (2023).
3. Guan, A. *et al.* Boosting CO₂ Electroreduction to CH₄ via Tuning Neighboring Single-Copper Sites. *ACS Energy Lett.* **5**, 1044–1053 (2020).
4. Kim, B. *et al.* Trace-Level Cobalt Dopants Enhance CO₂ Electroreduction and Ethylene Formation on Copper. *ACS Energy Lett.* **8**, 3356–3364 (2023).
5. Wei, S. *et al.* Construction of single-atom copper sites with low coordination number for efficient CO₂ electroreduction to CH₄. *J. Mater. Chem. A* **10**, 6187–6192 (2022).
6. Roy, S. *et al.* Cooperative Copper Single-Atom Catalyst in 2D Carbon Nitride for Enhanced CO₂ Electrolysis to Methane. *Adv. Mater.* **36**, 2300713 (2024).
7. Zou, Haiyuan, *et al.* Electronic Perturbation of Copper Single-Atom CO₂ Reduction Catalysts in a Molecular Way. *Angewandte Chemie* 135.6 (2023).